って聴力回復が起こることが示された。これらは高音域に聴力低下を残す不完全な自己聴力再生であるが、骨髄間葉系幹細胞による再生治療の検討では外側壁への生着が確認され、更に回復率の上昇が見られたことから、今後の検討により自己回復の困難な症例も含め、新規治療法として応用することが可能であると考えられる。

E. 結論

本研究では内耳エネルギー不全状態では、有毛細胞よりむしろ蝸牛外側壁やらせん板縁の蝸牛線維細胞が起因となって高度難聴が起こることが示され、蝸牛線維細胞の再生を新たなターゲットとして治療法の検討を行う必要があることが示された。

これらのことから内耳エネルギー不全が原因として疑われる突発性難聴の新規治療法として、半規管からの骨髄間葉系幹細胞の移植による蝸牛線維細胞の補充が今後有効な治療法の候補として期待できる。

F. 健康危険情報

なし

G. 研究発表

1. 論文発表

なし

2. 学会発表

神谷和作、保谷則之、岡本康秀、新田清一、中川進、藤井正人、松永達雄
演題名：内耳ミトコンドリア機能障害による難聴モデルラットの作成とその難聴の病態解析
第 51 回日本実験動物学会総会、長崎市、2004 年 5 月 21 日

Kamiya K, Hoya N, Okamoto Y, Fujinami Y, Komatsuzaki R, Kusano R, Nakagawa S, Fujii M, Matsunaga T, Regeneration of cochlear fibrocytes leads to hearing recovery in a rat model of acute cochlear mitochondrial dysfunction.
5th Molecular Biology of Hearing and Deafness, Bethesda, MD, USA, October 3rd, 2004

H. 知的財産権の出願・登録状況

なし

厚生労働科学研究費補助金（感覚器障害研究事業）
分担研究報告書

コネキシン蛋白の発現と細胞増殖・分化の検討

研究協力者　小沢宏之　国立病院機構東京医療センター耳鼻咽喉科
研究協力者　神谷和作　国立病院機構東京医療センター
臨床研究センター研究員
分担研究者　藤井正人　国立病院機構東京医療センター
臨床研究センター聴覚・平衡覚研究部長
主任研究者　松永達雄　国立病院機構東京医療センター
臨床研究センター聴覚障害研究室長

研究要旨

ギャップジャンクション蛋白であるコネキシンは人体の様々な臓器に発現し細胞間情報伝達の役割を果たしている。またコネキシンは難聴遺伝子の一つとしても知られており、蝸牛外側壁線維細胞で発現し、内耳でのイオン輸送に重要な働きをしていることが知られている。この線維細胞は、内耳エネルギー不全により細胞増殖が誘導される。我々は、蝸牛線維細胞の増殖とコネキシンとの関連を調べる前段階として、臨床検体を用い、正常組織と癌組織におけるコネキシン発現について比較した。その結果、周囲正常組織に比較し、腫瘍組織でのコネキシン蛋白の発現は低下していると考えられた。また腫瘍細胞にコネキシン遺伝子を導入し強制発現させした結果、コネキシン蛋白は膜ではなく細胞内に局在した。この結果は臨床検体の腫瘍細胞におけるコネキシン蛋白の局在に一致しており、細胞増殖にコネキシン蛋白が関連している可能性が高いと考えられた。今後、コネキシンが細胞増殖に関わるメカニズムを解明することで、コネキシンを用いた蝸牛線維細胞の遺伝子治療などの可能性が期待される。

A. 研究目的

コネキシンは、細胞間結合の一つであるギャップジャンクションを構成するタンパク質である。またコネキシンは遺伝子難聴の原因遺伝子の一つである。コネキシンは内耳エネルギー不全に最も感受性の高い蝸牛外側壁線維細胞で発現されており、内耳での

イオン輸送に重要な働きをしていることが知られている。この線維細胞は、我々の現在までの研究で、内耳エネルギー不全により細胞増殖が誘導されることがわかってきている。

一方で1990年頃より、癌組織においてコネキシン蛋白の発現が低下することが報告されるようになり、その意義について検討され始め、in vitroの実験系において、様々な腫瘍細胞へコネキシンが導入され、腫瘍細胞の増殖能力が抑制されることが報告されるようになった。その機序としては、ギャップジャンクションを介した隣接細胞から増殖抑制物質が細胞内に流入するという仮説がたてられていたが、最近になって、コネキシン蛋白が細胞周期に直接影響を与えるとする報告があり、コネキシンが細胞の増殖に深く関わりを持つ可能性が考えられている。

今回我々は、内耳エネルギー不全により生じる線維細胞の増殖とコネキシンとの関連を調べる前段階として、正常組織におけるコネキシン発現の動態と増殖が活性化した細胞、すなわち癌細胞におけるコネキシン発現とを比較した。この結果から腫瘍細胞へのコネキシン遺伝子の導入を行いその影響について検討を行った。

B. 研究方法

1．癌組織と正常組織におけるコネキシン蛋白の発現の検討

＜対象＞根治手術を行った頭頸部癌症例のうち本研究に摘出組織の一部を本研究に用いることに同意の得られた8例。原発巣の内訳は下咽頭癌4例、舌癌2例、喉頭癌1例、口腔底癌1例。全例扁平上皮癌であった。本研究は、臨床検体を用いるにあたり東京医療センター倫理委員会における審査され承認を得た。

＜方法＞根治手術により摘出した検体を用い、肉眼的に分かる範囲で正常組織と癌組織の境界を含むように組織を採取した。4%パラホルムアルデヒドで10～12時間固定した後、パラフィンに包埋した。切片を作成し、抗ウサギ抗コネキシン26（Cx26）抗体 および抗コネキシン 30(Cx30)抗体（Zymed社製）を用い、ABC法で免疫染色を行い、各コネキシンの分布を観察した。

mRNA 発現については、同じく根治手術後の検体を用い、腫瘍側および正常側より組織を採取した。これらの組織から Trizol を用いてtRNAを抽出しtRNAよりcDNAを作成した。Real Time PCR 法を用いて、各組織におけるコネキシンのmRNA を相対的に定量した。内因性コントロールとして GAPDH を

用いた。

2．腫瘍細胞へのコネキシン遺伝子の導入

HeLa 細胞を用いてコネキシン遺伝子の導入を行った。導入するコネキシンとしては遺伝難聴の原因遺伝子として知られているコネキシン26(Cx26)を用いた。

遺伝子導入は pcDNA3.1 プラスミドを用い。このプラスミドに human coxxexin26 遺伝子（hCx26）を組み込み、hCx26 と GFP（green fluorescent protein）の fusion protein を強制発現させるプラスミドを作成した。またコントロールとして、GFP のみを発現するプラスミドを作成した。

Lipofectamine を用いて HeLa 細胞に Cx26 を遺伝子導入し、その局在を蛍光顕微鏡で観察した。また増殖能をコントロールと比較した。

C. 研究結果

1．癌組織と正常組織におけるコネキシン蛋白の発現の検討

＜Cx26＞

- 正常側粘膜は、基底層の細胞から染色され全層がほぼ均一であった。
- 下咽頭癌の検体では腫瘍側では正常側と比較して染色が弱い傾向にあった。
- その他の検体（舌・喉頭・口腔底）では、免疫染色の結果では正常側と腫瘍側とで Cx26 発現を認め、明らかな差を認めなかった。
- 腫瘍内で Cx26 は点状に染色された。

＜Cx30＞

- 正常側粘膜では基底層の細胞は染色が弱く、有棘層に強く染色された。
- 喉頭の検体では基底層より強く染色された。
- 下咽頭の検体では、免疫染色の結果では正常側より腫瘍側で発現が多かった。
- 腫瘍内で Cx30 は主に細胞膜に染色された。
- その他の検体（舌・喉頭・口腔底）では、免疫染色の結果では正常側と腫瘍側との間で明らかな差がなかった。

＜mRNA＞

- 正常組織と腫瘍組織における Cx26 および Cx30 のmRNA の発現に明らかな傾向はなかった。

2．腫瘍細胞へのコネキシン遺伝子の導入

今回用いたプラスミドによる遺伝子導入では、Lipofectamine を用いることで、50%程度の細胞に遺伝子が導入されることを確認できた。強制発現

したCx26蛋白は、大部分は膜へ配置されずに細胞質内に存在した。

増殖能については、現時点で検討中であるが、Cx26導入細胞で増殖能が抑制されている印象があった。

D.考察

コネキシンは現時点で15種類以上が確認されており、臓器ごとに発現しているコネキシンの種類が異なる。特に、内耳ではCx26、Cx30が発現しており、これらのコネキシンは難聴遺伝子でもある。またCx26、Cx30は表皮・粘膜のケラチノサイトにも存在し、動物実験では皮膚や粘膜の癌化に伴いこれらのコネキシン蛋白の発現が減少することが報告されている。一方、マイクロアレイによる頭頸部癌のRNA発現の検討では腫瘍組織でCx26のRNA発現の増加を認めたとの報告もあり、細胞の癌化あるいは増殖にコネキシンが何らかの形で関わってきていることは想定されてきているものの、コネキシンの臓器特異的な発現や構成が解明されていないことや、各コネキシンの機能が判明していないことなどから、コネキシンによる細胞増殖への関与のメカニズムの詳細は未だ明らかにされていない。

今回の検討では正常上皮におけるコネキシン分布の差が明らかになった。すなわち、正常扁平上皮ではCx26は各層でほぼ均一に発現を認めたが、Cx30は基底層では発現が少なかった。また繊毛上皮を持つ喉頭ではCx30は基底層より発現を認めた。増殖の亢進した状態である腫瘍組織ではコネキシンの発現は減少する傾向があった。腫瘍細胞では同じコネキシンでもCx26では細胞質内に点状に存在し、Cx30は細胞膜に存在した。各コネキシン蛋白が増殖に伴う役割が異なる可能性があると考えられた。

腫瘍細胞にCx26を強制発現させた結果は現在も検討中であるが、蛍光顕微鏡での観察ではCx26は必ずしも細胞膜に局在せず、大部分が細胞質にあり、臨床検体で見られたCx26の分布と一致していると考えられた。

今後は各コネキシン蛋白の細胞殖への関与のメカニズムについて検討を行い、機能障害の生じた内耳における線維細胞の再生にコネキシンがどのように関わってくるのかを解明していく予定である。

E. 結論

頭頸部癌の周囲正常組織に比較し腫瘍組織でのコネキシン蛋白の発現は低下する傾向があると考えられた。また正常組織でもコネキシン蛋白の発現の分布が異なっていた。

腫瘍細胞にコネキシン遺伝子を導入し強制発現させた結果、コネキシ

ン蛋白は膜ではなく細胞内に局在した。この結果は臨床検体の腫瘍細胞におけるコネキシン蛋白の局在に一致しており、何らかの形で細胞増殖にコネキシン蛋白が関連している可能性が高いと考えられた。

F. 健康危険情報

なし

G. 研究発表

1. 論文発表

なし

2. 学会発表

なし

H. 知的財産権の出願・登録状況

なし

別紙４

研究成果の刊行に関する一覧表レイアウト

雑誌

発表者氏名	論文タイトル名	発表誌名	巻号	ページ	出版年
Hoya N, Okamoto Y, Kamiya K, Fujii M, Matsunaga T	A novel animal model of acute cochlear mitochondrial dysfunction.	Neuroreport	15(10)	1597-1600	2004
Okamoto Y, Hoya N, Kamiya K, Fujii M, Ogawa K, Matsunaga T	Permanent Threshold Shift Caused by Acute Cochlear Mitochondrial Dysfunction Is Primarily Mediated by Degeneration of the Lateral Wall of the Cochlea.	Audiol Neurootol	10(4)	220-233	2005

A novel animal model of acute cochlear mitochondrial dysfunction

Noriyuki Hoya, Yasuhide Okamoto, Kazusaku Kamiya, Masato Fujii and Tatsuo Matsunaga[CA]

Laboratory of Auditory Disorders, National Institute of Sensory Organs, National Tokyo Medical Center, 2-5-1 Higashigaoka, Meguro-ku, Tokyo 152-8902, Japan

[CA]Corresponding Author: matsunagatatsuo@kankakuki.go.jp

Received 28 March 2004; accepted 11 May 2004

DOI: 10.1097/01.wnr.0000133226.94662.80

Acute mitochondrial dysfunction in the cochlea is likely to result in hearing loss as a consequence of local energy shortage, similar to ischemia- or noise-induced hearing loss. To establish an animal model of acute cochlear mitochondrial dysfunction, we applied a mitochondrial toxin, 3-nitropropionic acid (3-NP) in the rat cochlea. Rats treated with 500 mM 3-NP exhibited permanent threshold shifts in acoustic brainstem response while the same volume of 300 mM 3-NP caused temporary threshold shifts. Histological examination in the permanent threshold shift model revealed severe degeneration of fibrocytes within spiral ligament and spiral limbus, indicating these cells are vulnerable to acute mitochondrial dysfunction. This model represents a novel tool for investigating the pathophysiology of acute cochlear mitochondrial dysfunction. *NeuroReport* 15:1597–1600 © 2004 Lippincott Williams & Wilkins.

Key words: Cochlea; Fibrocytes; Lateral wall; Mitochondria; 3-Nitropropionic acid; Potassium recycling; Temporary threshold shift

INTRODUCTION

Hearing loss is one of the most prevalent features of mitochondrial diseases [1]. The fact that mitochondrial DNA mutations frequently lead to hearing loss suggests that cochlear cells are strongly dependent upon mitochondrial function [2]. Because the majority of mitochondrial diseases are characterized by a deficiency of enzymes in the electron transport chain [3–5], a resultant reduction of ATP production may underlie the pathogenesis of sensorineural hearing loss that accompanies these diseases. In addition, mitochondrial dysfunction may mediate the pathogenesis of ischemia- and noise-induced hearing loss since decreased blood supply or excessive stimulation might cause local energy shortages [6]. Thus, mitochondrial dysfunction may underlie the pathogenesis of several types of sensorineural hearing loss related to energy failure.

The mitochondrial toxin 3-nitropropionic acid (3-NP) is an irreversible inhibitor of succinate dehydrogenase, and blocks complex II of the mitochondrial electron transport chain [7]. Systemic administration of 3-NP produces selective striatal legion damage and clinical features of Huntington's disease [8–10]. The effect of this agent in the cochlea can be regarded as insufficiency of cellular energy in the cochlea. In the present study, we investigated the effect of local application of 3-NP in rat to establish an animal model of acute mitochondrial dysfunction in the cochlea.

MATERIALS AND METHODS

Animals and surgery: Twenty-seven female Sprague–Dawley rats weighing 180–220 g were anesthetized with pentobarbital (30–40 mg/kg, i.p.) and an incision was made following local administration of lidocaine (1%). The left otic bulla was opened using the retroauricular approach. The end of PE 10 tubing (Becton Dickinson, NJ, USA) was drawn to a fine tip in a flame and gently inserted into the round window niche. 3-NP (Sigma, St. Louis, MO, USA) dissolved in saline (pH 7.4) was administered at 500 mM, 300 mM and 50 mM for 2 min at a rate of 1.5 µl/min with a syringe pump. Saline was used as a control. A tiny piece of gelatin was put on the niche and the wound was closed. The right cochlea was surgically destroyed to avoid cross hearing during auditory brainstem response (ABR) recording. Experimental procedures reported in this study were approved by the Institutional Animal Care and Use Committee of The National Tokyo Medical Center.

ABR recording: ABR was recorded before surgery and 1 and 3 h and 1, 3, 7, 14, 21 and 28 days after surgery using Scope waveform storing and stimulus control software and the PowerLab data acquisition and analysis system (PowerLab2/20, AD Instruments, Castle Hill, Australia). EEG recordings were acquired using the Digital Bioamp extracellular amplifier system (BAL-1, Tucker-Davis Technologies, FL, USA). Sound stimuli were produced by a coupler type speaker (ES1spc, Bio Research Center, Nagoya, Japan) inserted into the ear canal. Pure tone bursts of 8, 12, 16 and 20 kHz (0.2 ms rise/fall time and 1 ms flat segment) were generated and the amplitude specified by a real-time processor and programmable attenuator (RP2.1 and PA5, Tucker-Davis Technologies, FL, USA). Sound levels were calibrated using a sound level meter (NL32, RION, Tokyo,

Japan) and the maximum output level at each frequency was 93, 96, 80, 79 dB at 8, 12, 16, 20 kHz, respectively. For recording, the animals were anesthetized with pentobarbital before stainless steel needle electrodes were placed ventrolateral to the bilateral ears. Waveforms of 512 stimuli at a frequency of 9 Hz were averaged and the visual detection threshold was determined with increment or decrement of sound pressure level by 5 dB steps. The effect of 3-NP on the ABR threshold was analyzed by comparing the threshold in the presence of 3-NP to the control using two-way repeated measures ANOVA, followed by a multiple comparison procedure (Student-Newman-Keuls method). The significance level for all statistical procedures was set at $p<0.05$.

Histological analysis: Fourteen days after administration, control rats and the experimental rats treated with 50 mM or 500 mM 3-NP were deeply anesthetized with pentobarbital and transcardially perfused with 100 ml 0.01 M phosphate buffered saline (PBS) followed by 50 ml fixative consisting of freshly depolymerized 2% paraformaldehyde and 2.5% glutaraldehyde in 0.1 M PBS. Left temporal bones were removed and immediately placed in the fixative. Openings were made at the round window, oval window and the apex of the cochlea. After immersion in the same fixative overnight, cochleae were decalcified in 0.1 M EDTA with 5% sucrose for 6 days, rinsed in 0.1 M PBS overnight, and post-fixed in 1% osmium tetroxide for 150 min. They were then dehydrated in a graded ethanol series, embedded in Epon 812 resin, sectioned in a horizontal plane parallel to the modiolus at 12.5 μm, and stained with toluidine blue for light microscopic examination.

RESULTS

The ABR thresholds for all frequencies tested were significantly elevated 1 h after administration of either 500 mM or 300 mM 3-NP while the administration of 50 mM 3-NP or physiological saline did not result in a detectable threshold shift (Fig. 1). In the 500 mM group, ABR thresholds exceeded the maximum recording limit for all frequencies tested 3 h after administration and persisted for at least 28 days. In the 300 mM group, the ABR thresholds started to improve at all frequencies tested after 3 days and recovered to levels that were not significantly elevated at 8, 12 and 16 kHz in 14 days; however, they remained significantly elevated at 20 kHz even after 28 days. The average hearing improvement was 59, 66, 65 and 73 dB at 20, 16, 12 and 8 kHz, respectively.

In rats treated with 500 mM 3-NP, all structures in the apical turn and the spiral ganglion neurons in the modiolus were well preserved 14 days after administration. In the middle turn, the fibrocytes in the spiral ligament and spiral limbus exhibited substantial degenerative changes (Fig. 2c, Fig. 3c). In the spiral ligament, most types of fibrocytes were degenerated. Loss of type II fibrocytes was apparent around the spiral prominence and root cells appeared to have shrunk. Type IV fibrocytes in the basilar crest were conspicuously degenerated. Obvious changes were not detected within the stria vascularis by light microscopy. In the spiral limbus, loss of stellate fibrocytes of the limbic central zone was prominent while interdental cells in the same zone were normal. Degeneration of supralimbal fibrocytes was also detected with marked swelling of supralimbal epithelium. In contrast, hair cells, supporting cells and nerve fibers in the organ of Corti were well preserved (Fig. 3c). In the basal turn, fibrocytes in the spiral ligament and spiral limbus showed severe degeneration while cells in the organ of Corti and the stria vascularis showed only slight degeneration. In rats treated with control or 50 mM 3-NP, the cochlea showed a normal structure in all turns 14 days after administration (Fig. 2a,b, Fig. 3a,b).

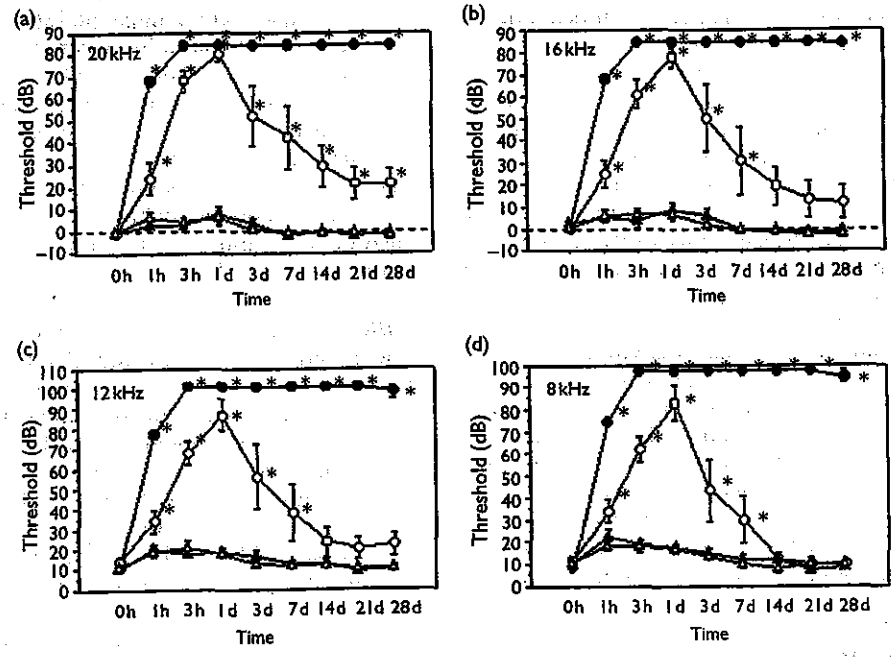

Fig. 1. The ABR threshold (dB SPL) before and after local administration of 3-NP (mean ± s.e.) at each frequency tested: (a) 20 kHz, (b) 16 kHz, (c) 12 kHz, (d) 8 kHz. Filled circles, open circles, filled triangles and open triangles indicate 500 mM (n=5), 300 mM (n=5), 50 mM (n=6), 3-NP and control groups (n=6), respectively. *$p<0.05$ vs controls (Student-Newman-Keuls multiple comparison procedure).

Fig. 2. Histological findings of the lateral wall in the cochlear middle turn 14 days after administration of control saline (a), 50 mM 3-NP (b), or 500 mM 3-NP (c). A normal structure was observed in the lateral wall of the control ear (a) and in that of the experimental ear treated with 50 mM 3-NP (b). (c) Upon administration of 500 mM 3-NP, loss and degeneration of fibrocytes were evident throughout the spiral ligament (black arrowheads). Loss of type II fibrocytes was prominent around the spiral prominence (white arrow), and root cells appeared shrunken (white arrowhead). Atrophy of type IV fibrocytes within the basilar crest was detected (black arrow). The *stria vascularis* was structurally well preserved. Toluidine blue stain. Bars=50 μm.

DISCUSSION

The present study demonstrates that cochlear mitochondrial dysfunction caused by administration of 3-NP results in hearing loss in a concentration-dependent manner, and the degree of hearing loss induced by different concentrations of 3-NP was well correlated with the extent of histological abnormality. Both the function and structure of the cochlea were normal in the rats treated with control saline or 50 mM 3-NP, indicating that the rat cochlea is tolerant to the effect of 50 mM 3-NP administration. However, administration of 300 mM 3-NP and 500 mM 3-NP induced temporary threshold shifts and permanent threshold shifts, respectively. Within the cochlea treated with 500 mM 3-NP, cellular damage was most prominent in the basal turn, intermediate in the middle turn, and minimal in the apical turn. Because 3-NP was applied from the round window and diffused in the perilymph, the difference in the damage by turns was most likely due to the different levels of exposure to 3-NP. Extreme susceptibility of cochlear fibrocytes to mitochondrial dysfunction is striking because the organ of Corti and/or stria vascularis are generally considered to be more susceptible to insults such as ischemia/hypoxia and noise and are essential for normal hearing [11,12].

The role of fibrocytes in the pathophysiology of sensorineural hearing loss is not fully understood. However, a number of recent studies have shown that degeneration of the cochlear fibrocytes could be a primary cause for some kinds of hearing loss. In a mouse model of aging, loss of fibrocytes within the spiral ligament was detected as the first morphological sign of cochlear degeneration [13], although another study using a gerbil model reported that these changes were secondary to dysfunction of the stria vascularis [14]. Extreme vulnerability of fibrocytes to noise insult was also reported in the mouse spiral ligament and spiral limbus [15]. Further study by the same group also revealed temporarily decreased endocochlear potential in the same experiment with a permanent threshold shift, suggesting reversible dysfunction of the lateral wall fibrocytes [16]. Furthermore, a mouse model of DFN3 nonsyndromic deafness exhibiting severe hearing loss had altered cochlear fibrocytes and decreased endocochlear potential [17].

Consistent with these reports, the degeneration of cochlear fibrocytes observed in this study might be the main cause for hearing loss in our experiments because the changes in the organ of Corti and the stria vascularis were minimal as observed by light microscopy. These cochlear fibrocytes are thought to play important roles in maintaining high K^+ concentrations in the endolymph by recycling K^+ from the perilymph [18,19]. The possible mechanism for ABR threshold elevation may be decreased K^+ concentration in the endolymph and resultant loss of endolymphatic potential. The slow recovery of ABR threshold observed in rats treated with 300 mM 3-NP suggests that these fibrocytes may regenerate as previously reported [20] and restore organ function. Since the possibility of slow hearing recovery is one of the remarkable clinical features in patients with acute sensorineural hearing loss, mitochondrial dysfunction in the cochlea may be one of the pathological pathways of such hearing impairment.

CONCLUSION

The present animal model of acute cochlear mitochondrial dysfunction exhibited either a permanent threshold shift, a temporary threshold shift, or normal hearing depending on

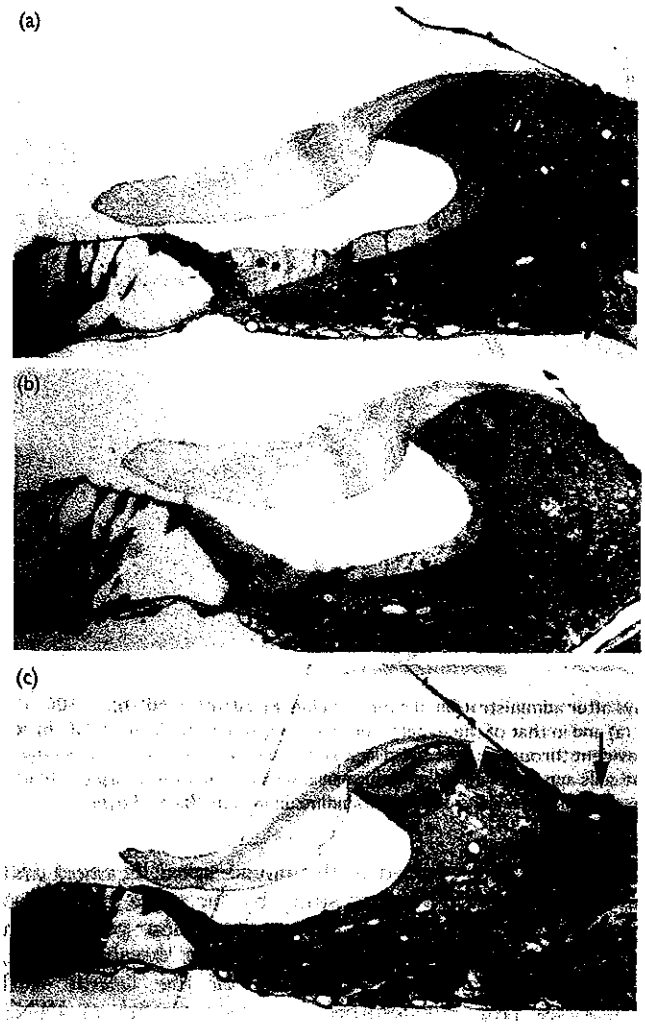

Fig. 3. Histological findings of the organ of Corti and spiral limbus in the cochlear middle turn 14 days after administration of control saline (a), 50 mM 3-NP (b), or 500 mM 3-NP (c). A normal structure was observed in the organ of Corti and spiral limbus of the control ear (a) and in those of the experimental ear treated with 50 mM 3-NP (b). (c) Upon administration of 500 mM 3-NP, loss of stellate fibrocytes was prominent in the limbic central zone (white arrow) while interdental cells appeared normal. Swelling of supralimbal fibrocytes (black arrow) was prominent. The organ of Corti was structurally well preserved. Toluidine blue stain. Bars=50 μm.

the amount of 3-NP administered into the cochlea, and these functional changes were well correlated with the histological changes in the cochlea. This model revealed the extreme vulnerability of cochlear fibrocytes to mitochondrial dysfunction and is likely to contribute to further understanding of the pathophysiology of acute sensorineural hearing loss.

REFERENCES

1. Gold M and Rapin I. Non-Mendelian mitochondrial inheritance as a cause of progressive genetic sensorineural hearing loss. *Int J Pediatr Otolaryngol* 1994; 30:91–104.
2. Hutchin TP and Cortopassi GA. Mitochondrial defects and hearing loss. *Cell Mol Life Sci* 2000; 57:1927–1937.
3. Goto Y, Horai S, Matsuoka T, Koga Y, Nihei K, Kobayashi M *et al.* Mitochondrial myopathy, encephalopathy, lactic acidosis, and stroke-like episodes (MELAS): a correlative study of the clinical features and mitochondrial DNA mutation. *Neurology* 1992; 42:545–550.
4. Wallace DC, Zheng XX, Lott MT, Shoffner JM, Hodge JA, Kelley RI *et al.* Familial mitochondrial encephalomyopathy (MERRF): genetic, pathophysiological, and biochemical characterization of a mitochondrial DNA disease. *Cell* 1988; 55:601–610.
5. Degoul F, Nelson I, Lestienne P, Francois D, Romero N, Duboc D *et al.* Deletions of mitochondrial DNA in Kearns-Sayre syndrome and ocular myopathies: genetic, biochemical and morphological studies. *J Neurol Sci* 1991; 101:168–177.
6. Seidman MD, Quirk WS and Shirwany NA. Mechanisms of alterations in the microcirculation of the cochlea. *Ann NY Acad Sci* 1999; 884:226–232.
7. Alston TA, Mela I and Bright HJ. 3-Nitropropionate, the toxic substance of Indigofera, is a suicide inactivator of succinate dehydrogenase. *Proc Natl Acad Sci USA* 1977; 74:3767–3771.
8. Hamilton BF and Gould DH. Nature and distribution of brain lesions in rats intoxicated with 3-nitropropionic acid: a type of hypoxic (energy deficient) brain damage. *Acta Neuropathol (Berl)* 1987; 72:286–297.
9. Brouillet E, Hantraye P, Ferrante RJ, Dolan R, Leroy-Willig A, Kowall NW *et al.* Chronic mitochondrial energy impairment produces selective striatal degeneration and abnormal choreiform movements in primates. *Proc Natl Acad Sci USA* 1995; 92:7105–7109.
10. Sato S, Gobbel GT, Honkaniemi J, Li Y, Kondo T, Murakami K *et al.* Apoptosis in the striatum of rats following intraperitoneal injection of 3-nitropropionic acid. *Brain Res* 1997; 745:343–347.
11. Shulman JB, Lambert PR and Goodhill V. Acoustic Trauma- and noise-induced hearing loss. In: Canalis RF and Lambert PR (eds). *The Ear. Comprehensive Otology.* Philadelphia: Lippincott Williams & Wilkins; 2000, pp. 773–783.
12. Martini A and Silvano P. Disorders of the inner ear in adults. In: Luxon LM, Furman JM, Martini A and Stephens D (eds). *Text Book of Audiological Medicine. Clinical Aspects of Hearing and Balance.* London: Martin Dunitz; 2003, pp. 451–475.
13. Hequembourg S and Liberman MC. Spiral ligament pathology: a major aspect of age-related cochlear degeneration in C57BL/6 mice. *J Assoc Res Otolaryngol* 2001; 2:118–129.
14. Spicer SS and Schulte BA. Spiral ligament pathology in quiet-aged gerbils. *Hear Res* 2002; 172:172–185.
15. Wang Y, Hirose K and Liberman MC. Dynamics of noise-induced cellular injury and repair in the mouse cochlea. *J Assoc Res Otolaryngol* 2002; 3:248–268.
16. Hirose K and Liberman MC. Lateral wall histopathology and endocochlear potential in the noise-damaged mouse cochlea. *J Assoc Res Otolaryngol* 2003; 4:339–352.
17. Minowa O, Ikeda K, Sugitani Y, Oshima T, Nakai S, Katori Y *et al.* Altered cochlear fibrocytes in a mouse model of DFN3 nonsyndromic deafness. *Science* 1999; 285:1408–1411.
18. Schulte BA and Steel KP. Expression of alpha and beta subunit isoforms of Na,K-ATPase in the mouse inner ear and changes with mutations at the Wv or Sld loci. *Hear Res* 1994; 78:65–76.
19. Spicer SS and Schulte BA. Evidence for a medial K^+ recycling pathway from inner hair cells. *Hear Res* 1998; 118:1–12.
20. Roberson DW and Rubel EW. Cell division in the gerbil cochlea after acoustic trauma. *Am J Otol* 1994; 15:28–34.

Acknowledgements: The authors thank Mr Susumu Nakagawa for his technical support in the histological study. This study was supported by Health Science Research Grant from the Ministry of Health Labor and Welfare of Japan to T.M.

BOIS:AUD:ZAUDO340XA.93 FF: ZUP9 E1: 11.1.2004

Original Paper

Audiology & Neuro-Otology

Audiol Neurootol 340
DOI: 10.1159/0000XXXXX

Received: March 3, 2004
Accepted after revision: December 3, 2004
Published online: ■

Permanent Threshold Shift Caused by Acute Cochlear Mitochondrial Dysfunction Is Primarily Mediated by Degeneration of the Lateral Wall of the Cochlea

Yasuhide Okamoto[a] Noriyuki Hoya[a] Kazusaku Kamiya[a] Masato Fujii[a]
Kaoru Ogawa[b] Tatsuo Matsunaga[a]

[a]Laboratory of Auditory Disorders, National Institute of Sensory Organs, National Tokyo Medical Center, and
[b]Department of Otolaryngology, School of Medicine, Keio University, Tokyo, Japan

Key Words
3-Nitropropionic acid · Cochlea · Spiral prominence · Spiral ligament · Stria vascularis · Mitochondrial dysfunction · Permanent threshold shift · Rat

Abstract
Mitochondrial dysfunction in the cochlea is thought to be an important cause of sensorineural hearing loss. Recently, we have established a novel rat model with acute hearing impairment caused by exposure to the mitochondrial toxin 3-nitropropionic acid (3-NP) to analyze the mechanism of cochlear mitochondrial dysfunction. Both permanent and temporary threshold shifts were observed in this model depending on the amount of 3-NP used to induce hearing impairment. In this study, we demonstrate cochlear morphological changes in the permanent threshold shift model. Marked degeneration was detected in type 2 fibrocytes in the spiral prominence, type 4 fibrocytes in the spiral ligament, marginal cells and intermediate cells in the stria vascularis 3 h after 3-NP administration; these changes were progressive for at least 14 days. Less prominent degeneration was detected in type 1 and type 3 fibrocytes in the spiral ligament. These results indicate that permanent threshold shift caused by acute cochlear mitochondrial dysfunction is primarily mediated by cellular degeneration in the lateral wall of the cochlea, and suggest that therapy of cochlear hearing loss due to acute energy failure may be achieved through protection and regeneration of the cochlear lateral wall.

Introduction

Many mutations in mitochondrial DNA cause both nonsyndromic and syndromic sensorineural hearing loss [Hutchin and Cortopassi, 2000] that are primarily caused by cochlear dysfunction [Braverman et al., 1996; Sue et al., 1998; Yamasoba et al., 1996]. These facts suggest that cochlear cells are strongly dependent on mitochondrial function to maintain normal hearing. The most important cell physiological role of mitochondria is in oxidative

KARGER
Fax + 41 61 306 12 34
E-Mail karger@karger.ch
www.karger.com

1420–3030/05/0000–0000$22.00/0

Accessible online at:
www.karger.com/aud

T. Matsunaga, MD, PhD
Laboratory of Auditory Disorders, National Institute of Sensory Organs
National Tokyo Medical Center, 2-5-1 Higashigaoka, Meguro
Tokyo 152-8902 (Japan)
Tel. +81 3 3411 0111, Fax +81 3 3412 9811, E-Mail matsunagatatsuo@kankakuki.go.jp

phosphorylation to produce ATP, the primary source of cellular energy [Nicholls and Budd, 2000]. Mitochondria also function to integrate apoptotic pathways and to produce reactive oxygen species that cause cell damage [Green and Reed, 1998]. Both apoptosis and formation of reactive oxygen species have been reported to be involved in pathophysiological mechanisms of cochlear damage by ischemia, ototoxins, and noise [Huang et al., 2000; Yamane et al., 1995]. Thus, mitochondrial dysfunction is likely to play a critical role not only in hearing loss resulting from mitochondrial DNA mutations but also in other types of hearing loss.

To explore the effect of acute mitochondrial dysfunction in the cochlea, we established an animal model of acute cochlear energy failure by administering the mitochondrial toxin 3-nitropropionic acid (3-NP) into the rat round window niche [Hoya et al., 2004]. 3-NP is an irreversible inhibitor of succinate dehydrogenase, a complex II enzyme of the mitochondrial electron transport chain [Alston et al., 1977; Coles et al., 1979]. Systemic administration of 3-NP produces selective striatal lesion damage [Brouillet et al., 1995; Hamilton and Gould, 1987]. In our model, rats treated with 500 m*M* 3-NP exhibited a permanent threshold shift as measured by auditory brainstem response (ABR) while the same volume of 300 m*M* 3-NP caused only a temporary threshold shift [Hoya et al., 2004]. In the permanent threshold shift model, no response was detected by ABR using the maximal stimulus intensity for all tested frequencies (8, 12, 16, 20 kHz) 3 h after 3-NP administration, and this condition persisted for at least 28 days. In the temporary threshold shift model, the ABR thresholds deteriorated to the highest degree (approximately 80 dB SPL) at 1 day and recovered to normal levels at most frequencies in 14 days, although the ABR thresholds at 20 kHz remained significantly elevated (approximately 20 dB SPL) compared to the control even at 28 days [Hoya et al., 2004]. In the present study, we investigated structural and ultrastructural changes of the cochlea at various time points after 3-NP administration in the permanent threshold shift model.

Materials and Methods

Animals and Surgery

Experimental procedures reported in this study were approved by the Institutional Animal Care and Use Committee of the National Tokyo Medical Center. Female Sprague-Dawley rats weighing between 180 and 210 g (8–10 weeks old) were used. Before surgery, the animals were anesthetized with pentobarbital (30–40 mg/kg, i.p.) and an incision was made posterior to the left pinna near the external meatus after local administration of lidocaine (1%). The left otic bulla was opened to approach the round window niche. The end of PE 10 tubing (Becton Dickinson, N.J., USA) was drawn to a fine tip in a flame and gently inserted into the round window niche. 3-NP (Sigma, St. Louis, Mo., USA) was dissolved in saline at 500 m*M* and the pH was adjusted to 7.4 with NaOH. Saline alone was used as a control. The solution was administered for 2 min at a rate of 1.5 µl/min with a syringe pump. Following treatment, a tiny piece of gelatin was placed on the niche in order to keep the solution in the niche regardless of the head movement after awakening from anesthesia and the wound was closed. The right cochlea was surgically destroyed to avoid cross-hearing during ABR recording.

Histological Analysis

Histological analysis was performed at 3 h, 1 day, 7 days, and 14 days after 3-NP or saline administration (2 rats per time point). To confirm the level of hearing loss, ABR recording was performed before surgery, 3 h after 3-NP or saline administration and before transcardial perfusion for histological analysis at the end of the observation period (3 h, 1 day, 7 days, and 14 days after the administration) in each rat. Details of the method for ABR recording were described previously [Hoya et al., 2004]. Two untreated rats with normal hearing confirmed by ABR were also histologically analyzed as an additional control set. For fixation, rats treated with 3-NP as well as control rats were deeply anesthetized with pentobarbital and transcardially perfused with 0.01 *M* phosphate buffer (pH 7.4) containing 8.6% sucrose followed by fixative consisting of freshly depolymerized 2% paraformaldehyde and 2.5% glutaraldehyde in 0.1 *M* phosphate buffer (pH 7.4) containing 5% sucrose. After decapitation, left temporal bones were removed and immediately placed in the same fixative. Small openings were made at the round window, oval window and the apex of the cochlea. After immersion in the fixative overnight, the temporal bones were decalcified by placement in 0.1 *M* ethylene diamine tetra-acetic acid (pH 7.4) containing 5% sucrose that was stirred at 4°C for 6 days. The bones were then rinsed overnight in 0.1 *M* phosphate buffer containing 5% sucrose, postfixed in 1% osmium tetroxide in the same buffer for 150 min, dehydrated in a graded ethanol series, and embedded in Epon 812 resin. For light microscopy, semi-thin sections were cut in a horizontal plane parallel to the modiolus and stained with toluidine blue. The mean area of each spiral ganglion cell was measured in treated rats at each time point following the administration of 3-NP or control saline as well as in normal rats that did not receive any treatment. Measurements were based on 3 sections including the modiolus from each cochlea. First, images of spiral ganglia were taken with a light microscope (Eclipse E600; Nikon, Tokyo, Japan) equipped with a digital camera (PDMC-3; Nihon Poladigital, Tokyo, Japan). Second, the area of each individual spiral ganglion cell with a visible nucleus was measured in each section using digital image analysis software (MicroAnalyzer, Nihon Poladigital). For rats treated with control saline, the total number of spiral ganglion cells analyzed at each time point varied from 70 to 131 (mean: 97.5). For rats treated with 3-NP, the total number of spiral ganglion cells analyzed at each time point varied from 76 to 102 (mean: 89.8). In normal rats without any treatment, the total number of analyzed spiral ganglion cells was 101. For the statistical evaluation, the mean areas of spiral ganglion cells in rats treated with 3-NP and control saline were compared at each time point by the unpaired t test. Then, the mean areas of spiral ganglion cells in the normal rats and in rats treated with 3-NP were compared

by analysis of variance followed by the multiple comparison method.

For transmission electron microscopy, thin sections were cut at the apical side of the second turn, double-stained with lead citrate and uranyl acetate, and examined with a Hitachi H600 electron microscope. Because of the technical reason in cutting thin sections, ultrastructural observation was restricted to the organ of Corti, spiral prominence, stria vascularis, and a lower half of the spiral ligament which exhibited the most significant structural changes by light microscopy.

Results

General Structural Features of the Cochlea

The cochlear structures of both the experimental and control rats were examined at different time points following treatment. In these rats, no responses could be detected by ABR at 3 h after 3-NP administration using the maximal intensity at each tested frequency, and no recovery was observed thereafter. A typical tracing of the ABR result is shown in figure 1. Control rats did not exhibit a threshold shift following saline administration.

By light microscopy, there was a basal-to-apical gradient in the extent of cochlear damage in the rats treated with 3-NP, and the structural changes were most evident in the lateral wall in the middle and basal turns with lesser changes in the organ of Corti and modiolus. All structures in the apical turn were well preserved throughout the observation period. In the basal turn, inner and outer hair cells showed mild structural changes at 3 h after 3-NP administration, and these changes became severe by 7 days after administration. Supporting cells in the organ of Corti showed only mild degenerative changes throughout the observation period. The spiral ligament first exhibited mild structural changes at 3 h after 3-NP administration and the changes became severe at 7 days after administration. The stria vascularis exhibited mild structural changes at 7 days after 3-NP administration and became moderate at 14 days after administration. The structure of spiral ganglion cells remained normal during the observation period.

Although the histological changes were more severe and rapid in the basal portion of the cochlea, commonly recognized patterns of histological features were observed in both the middle and basal turns. Because of the relatively slow progression of histological changes in the apical side of the middle turn, we were able to analyze the process of morphological change in detail over time in this area. Thus, in the following sections, we describe the details of structural and ultrastructural changes of the cochlea at the apical side of the middle turn at various time points following 3-NP administration. There was little variation in the morphological findings between the 2 rats at each time point in both the experimental group and control group.

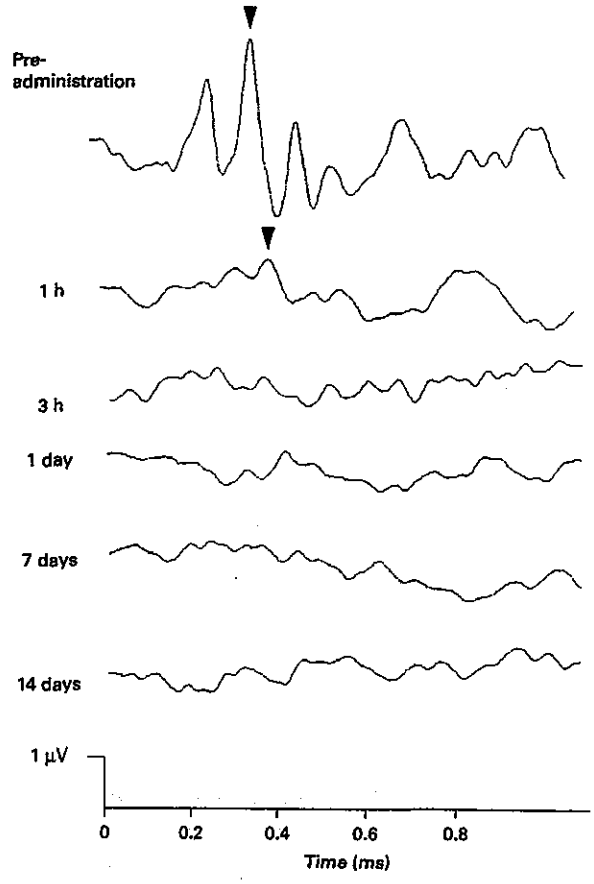

Fig. 1. A typical tracing of ABR results showing changes after administration of 3-NP. The stimuli consisted of pure tone bursts of 20 kHz and were delivered at 79 dB. Time after administration is indicated to the left of each tracing. Arrowheads indicate wave II. An additional recording 1 h after 3-NP administration is included to show the changes more clearly in this animal model.

Structural Changes in the Lateral Wall

Light microscopy revealed the enlarged extracellular spaces of the spiral prominence 3 h after 3-NP administration (fig. 2b). At 1 day after 3-NP administration, the extracellular spaces of the spiral ligament were also enlarged (fig. 2c), which became more apparent 7 days after

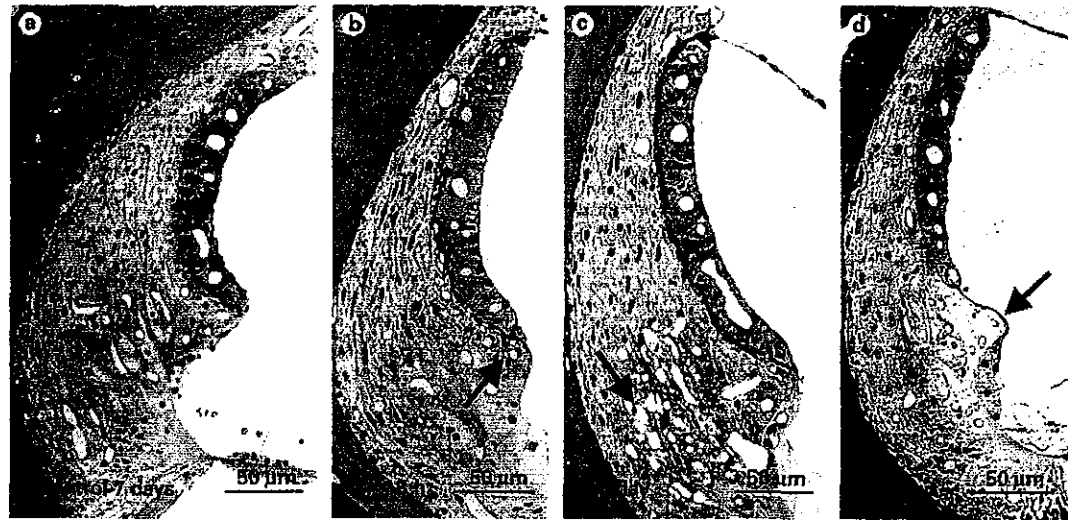

Fig. 2. Light microscopy of the cochlear lateral wall after the administration of control saline (**a**) or 3-NP (**b–d**). **a** Normal morphology at 7 days after saline administration. **b** At 3 h after 3-NP administration, the extracellular space in the spiral prominence was slightly enlarged (arrow). **c** At 1 day after 3-NP administration, the extracellular space in the spiral ligament was also remarkably enlarged (arrow). **d** At 14 days after 3-NP administration, fibrocyte loss was conspicuous in the spiral prominence (arrow).

the administration, and the majority of spiral prominence fibrocytes disappeared by 14 days following administration (fig. 2d). These histological changes were not observed in the control rats at any time point (fig. 2a). In the stria vascularis, no morphological changes were detected by light microscopy within the observation period after 3-NP administration in the experimental rats (fig. 2b–d) or saline treatment in the control rats (fig. 2a).

Fibrocytes of the spiral ligament are divided into 4 cell types based on structural features, immunostaining patterns and general location [Spicer and Schulte, 1996]. The classification is summarized in a scheme (fig. 3), and the following transmission electron microscopic findings are described according to this classification. Atrophy of type 2 fibrocytes and the enlargement of extracellular spaces in the spiral prominence were detected at 3 h after 3-NP administration (fig. 4b), which became more pronounced over time during the observation period. Nearly total loss of type 2 fibrocytes was noted at 14 days (fig. 4c). In contrast, spiral prominence capillaries and epithelia were maintained. In control rats, type 2 fibrocytes maintained normal morphology in that they contained numerous mitochondria and presented interdigitated cellular processes that were closely apposed by gap junctions (fig. 4a).

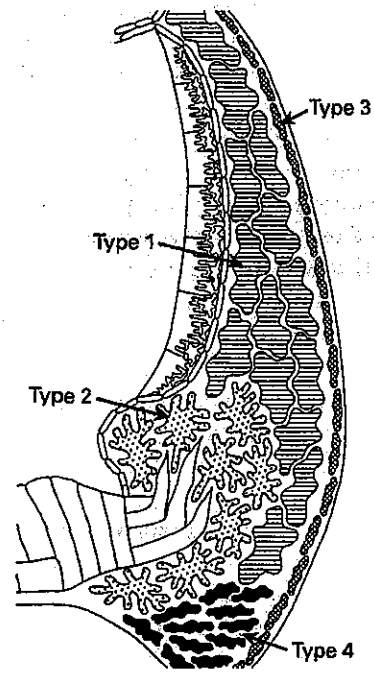

Fig. 3. Summary diagram of the lateral wall indicating the spatial relationship of the 4 types of fibrocytes in the spiral ligament.

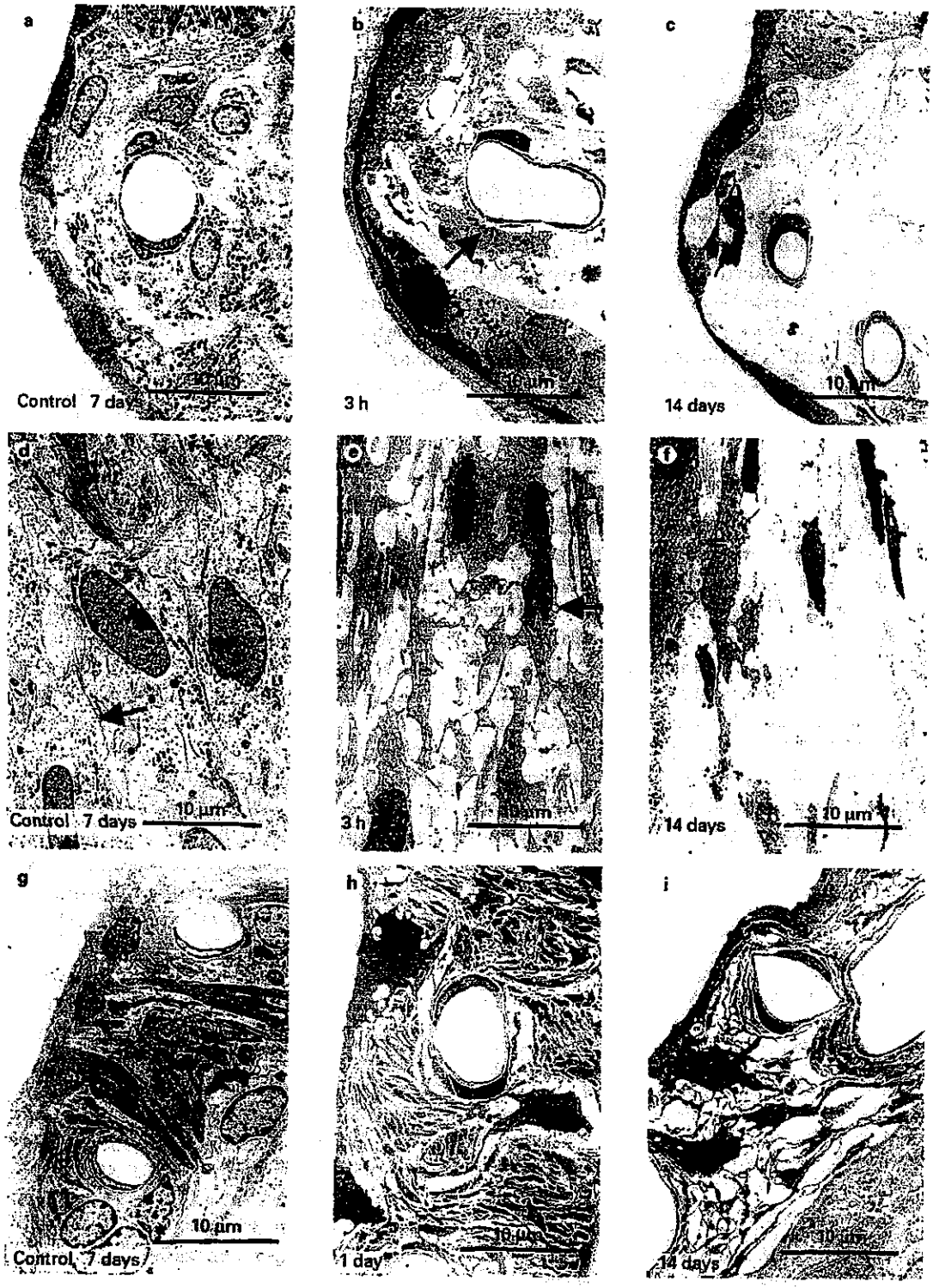
a
Control 7 days
b
3 h
c
14 days
d
Control 7 days
10 µm
e
3 h
f
14 days
10 µm
g
10 µm
Control 7 days
h
1 day
i
14 days

Type 4 fibrocytes in the lateral basal part of the spiral ligament also exhibited severe atrophy, and the extracellular space was enlarged 3 h after 3-NP administration in this area (fig. 4e). Mitochondrial swelling and nuclear atrophy were also apparent in these fibrocytes. Degenerative changes of type 4 fibrocytes progressed with time during the observation period. The enlargement of extracellular spaces and loss of fibrocytes were conspicuous 14 days after 3-NP administration (fig. 4f). Type 4 fibrocytes in the control rats exhibited normal morphology with modest cellular processes apposed by gap junctions and abundant mitochondria (fig. 4d).

Type 1 and type 3 fibrocytes in the spiral ligament also exhibited cellular atrophy 3 h after 3-NP administration, but the observed changes were milder than those in type 2 and type 4 fibrocytes. These changes remained unchanged during the observation period. No changes were detected in the corresponding cells in the control rats.

In the stria vascularis, marginal cells and intermediate cells exhibited progressive morphological changes, while capillaries and basal cells maintained normal morphology. At 3 h after 3-NP administration, the extracellular space between intermediate and marginal cells (i.e., the intrastrial space) was enlarged and became more pronounced over time. Marginal cells exhibited cellular atrophy associated with intracellular deposits and vacuolation 1 day after 3-NP administration (fig. 4h), as well as atrophy of the basolateral infoldings and loss of mitochondria at 7 days and nuclear atrophy at 14 days after treatment (fig. 4i). Intermediate cells exhibited cellular atrophy and vacuolation 1 day after 3-NP administration (fig. 4h), and nuclear atrophy 14 days after treatment (fig. 4i). In control rats, normal cellular structures of the stria vascularis were maintained, presenting with interdigitated basolateral infoldings of marginal cells containing numerous mitochondria, intermediate cells with tangled processes, and basal cells closely apposed to surrounding cells, and very narrow intrastrial space (fig. 4g).

Fig. 4. Transmission electron microscopy of the cochlear lateral wall after saline (**a**, **d**, **g**) or 3-NP (**b**, **c**, **e**, **f**, **h**, **i**) administration. **a** Normal cellular structures in the spiral prominence 7 days after saline administration. **b** Atrophy of type 2 fibrocytes with reduced numbers of mitochondria (arrow) and enlargement of the extracellular space were noted at 3 h after 3-NP administration. **c** Loss of type 2 fibrocytes was evident 14 days after 3-NP administration. **d** Normal morphology of type 4 fibrocytes connected by a gap junction (arrow) in the spiral ligament 7 days after saline administration. **e** Atrophy of type 4 fibrocytes with mitochondrial vacuolation (arrow) and enlargement of the extracellular space were prominent 3 h after 3-NP administration. **f** Loss of type 4 fibrocytes was conspicuous 14 days after 3-NP administration. **g** Normal morphology of stria vascularis at 7 days after saline administration. **h** Marginal cells appeared atrophic and contained intracellular deposits and vacuolation 1 day after 3-NP administration. Enlargement of the intrastrial space and atrophy of intermediate cell were also evident. **i** The intrastrial space was severely enlarged and marginal and intermediate cells exhibited both cellular and nuclear atrophy 14 days after 3-NP administration.

Structural Changes in the Organ of Corti

Light microscopy showed that the organ of Corti was structurally well preserved at all time points following 3-NP administration (fig. 5b–d). Significant degenerative changes were not observed in the inner hair cells and their innervation. Only slight shrinkage of the Deiters cells was detected 14 days after treatment (fig. 5d). In control rats, normal structures were maintained during the observation period (fig. 5a).

Ultrastructural analysis of the hair cells revealed translocation of mitochondria within outer hair cells. The mitochondria were located along the subsurface cisterns parallel to the lateral membrane at 3 h and 1 day after 3-NP administration (fig. 6b) as in control rats during the observation period (fig. 6a). However, the mitochondria were observed in the center of the outer hair cell cytoplasm at 7 days and 14 days after 3-NP administration (fig. 6c). Otherwise, outer hair cells including synapses appeared normal during the observation period. Inner hair cells exhibited normal ultrastructure including afferent and efferent nerve endings at all time points following saline administration in the control rats (fig. 6d). The same ultrastructural features were also observed in the inner hair cells at all time points following 3-NP administration in the experimental rats (fig. 6e, f).

Structural Changes in the Spiral Ganglion

Under light microscopy, spiral ganglion cells appeared structurally unchanged after either 3-NP administration in the experimental rats (fig. 7b–d) or saline treatment in the control rats (fig. 7a). Comparison of the area of spiral ganglion cells in rats treated with 3-NP and control saline at each time point revealed that the area in rats treated with 3-NP (mean ± SD: 207.8 ± 40.7 μm^2) was significantly different from the area in control rats (228.7 ± 45.7 μm^2) only at 3 h after administration ($p = 0.05$). However, the mean area of spiral ganglion cells at 3 h after 3-NP administration was not significantly different from the mean area of these cells in normal, untreated rats (224.1 ± 46.8 μm^2; $p = 0.05$).

Ultrastructural analysis revealed that almost all mitochondria in the spiral ganglion cells exhibited marked

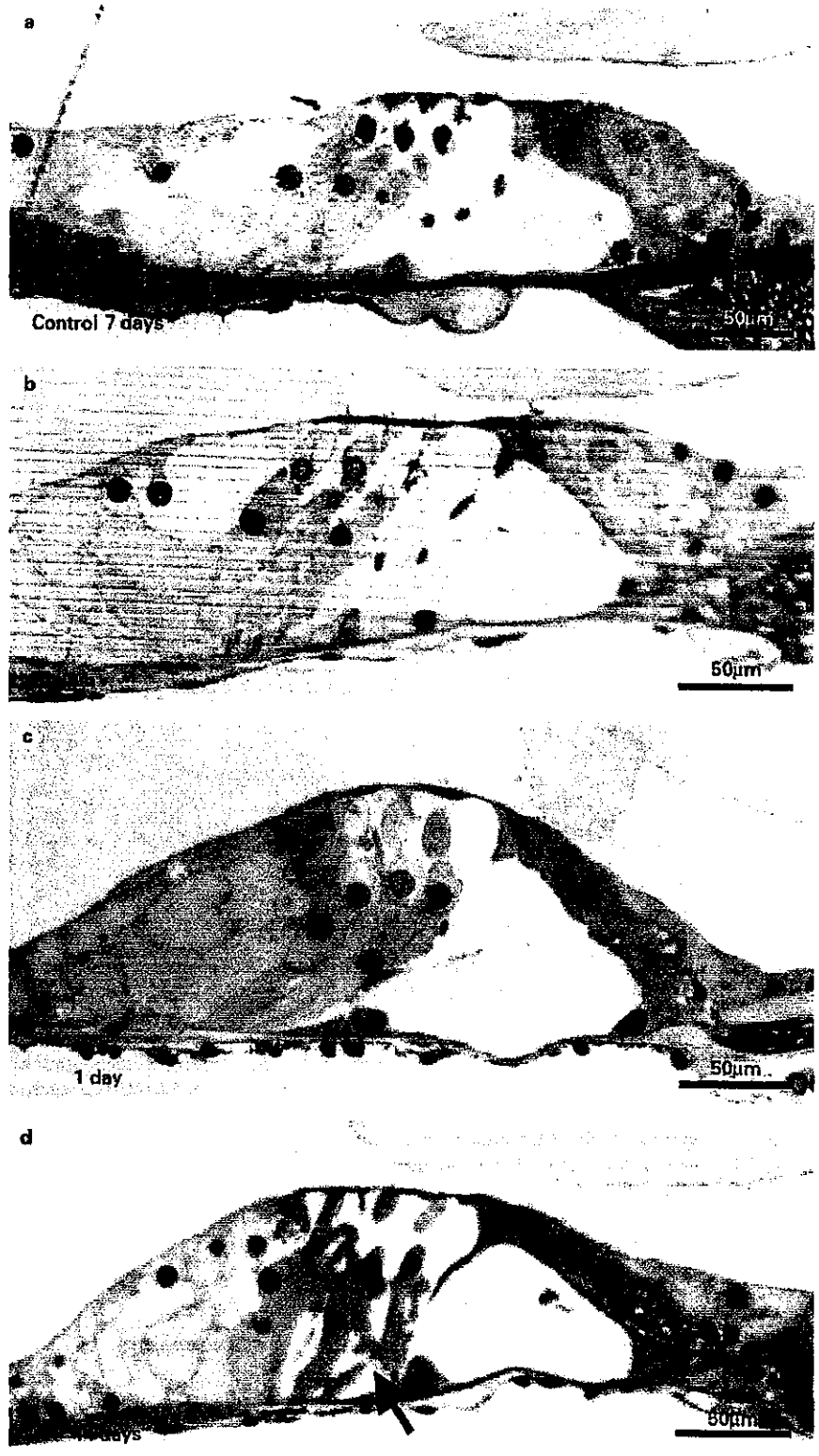

Fig. 5. Light microscopy of the organ of Corti after the administration of saline (**a**) or 3-NP (**b**, **c**, **d**). Normal morphology of the organ of Corti 7 days after saline administration (**a**), and at 3 h (**b**) and 1 day (**c**) after 3-NP administration. The organ of Corti exhibited slight shrinkage of the Deiters cells (arrow) but otherwise maintained normal structure 14 days after 3-NP administration (**d**).

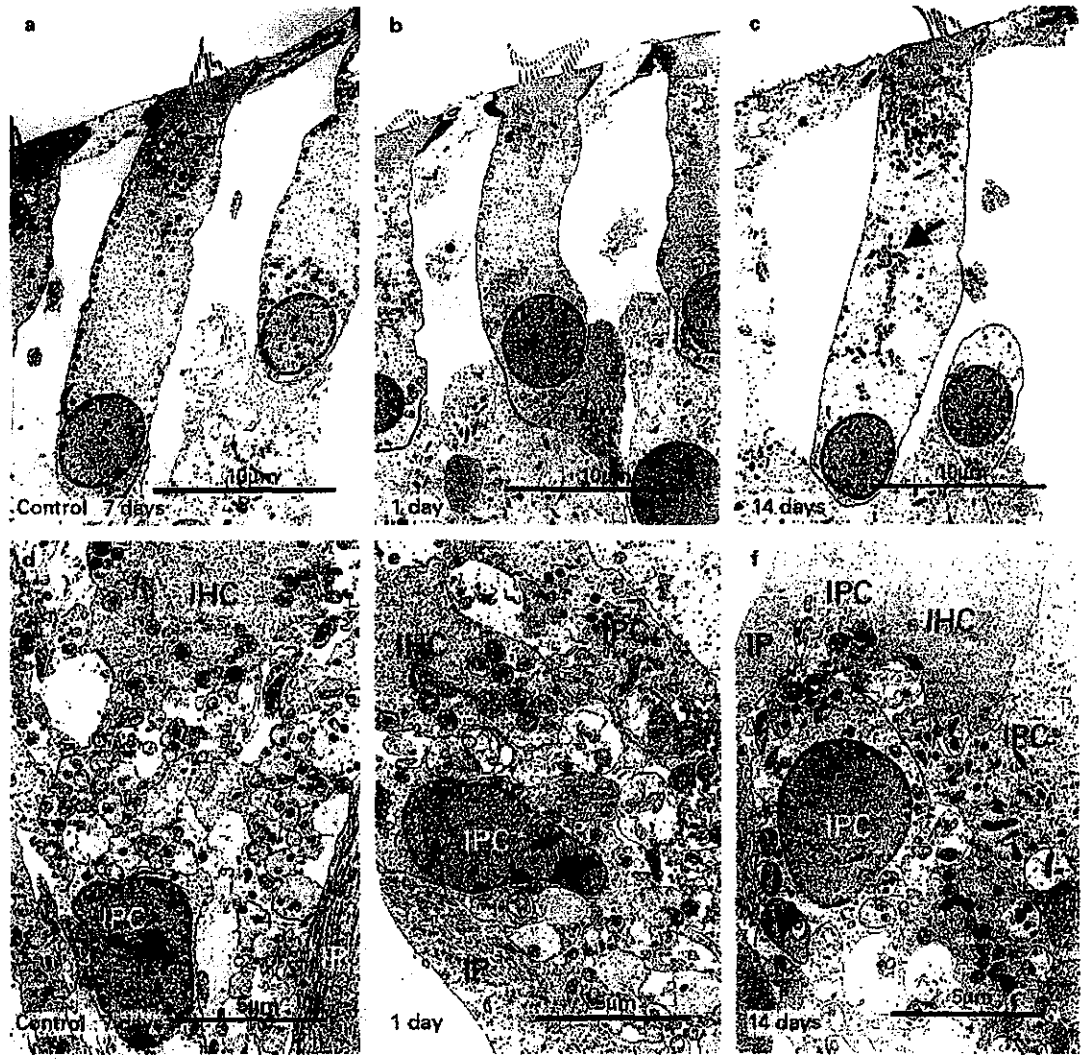

Fig. 6. Ultrastructural analysis of hair cells after the administration of saline (**a**, **d**) or 3-NP (**b**, **c**, **e**, **f**). **a** Normal structures in outer hair cells 7 days after saline administration. Mitochondria were distributed along the lateral wall of outer hair cells. **b** At 1 day after 3-NP administration, outer hair cells appeared structurally normal. **c** At 14 days after 3-NP administration, translocation of mitochondria into the center of cytoplasm (arrow) was noted. **d** Normal nerve endings 7 days after saline administration. Numerous nerve endings were seen at the bottom of the inner hair cell (IHC), and surrounded by the inner phalangeal cell (IPC) and the inner pillar cell (IP). At 1 day (**e**) and 14 days (**f**) after 3-NP administration, numerous nerve endings with the same structural features seen in the saline control were maintained at the bottom of the inner hair cell (IHC) and surrounded by the inner phalangeal cell (IPC) and the inner pillar cell (IP).

swelling 3 h after 3-NP administration (fig. 8b). The mitochondrial swelling became less apparent at 1 day following treatment. At 7 and 14 days, the structures appeared normal (fig. 8c). No ultrastructural changes were observed in the spiral ganglion cells of control rats (fig. 8a).

The structural changes observed in the cochlea following 3-NP administration are summarized in table 1.

Discussion

In the present study, we demonstrated that cellular degeneration in the lateral wall is the most remarkable change within the cochlea in response to acute mitochondrial dysfunction. The main physiological function of the cochlear lateral wall is ion transport and the generation of

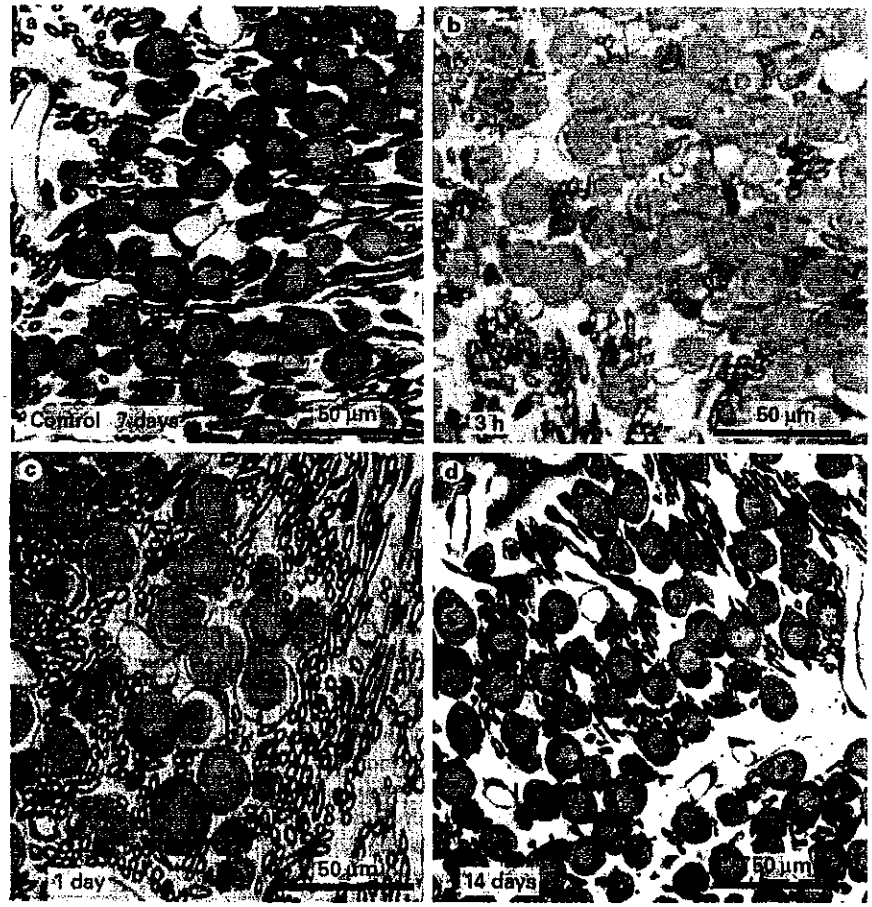

Fig. 7. Light microscopy of the spiral ganglion cells after administration of saline (**a**) or 3-NP (**b**, **c**, **d**). **a** Normal morphology in spiral ganglion cells 7 days after saline administration. At 3 h (**b**), 1 day (**c**), and 14 days (**d**) after 3-NP administration, spiral ganglion cells displayed normal structures.

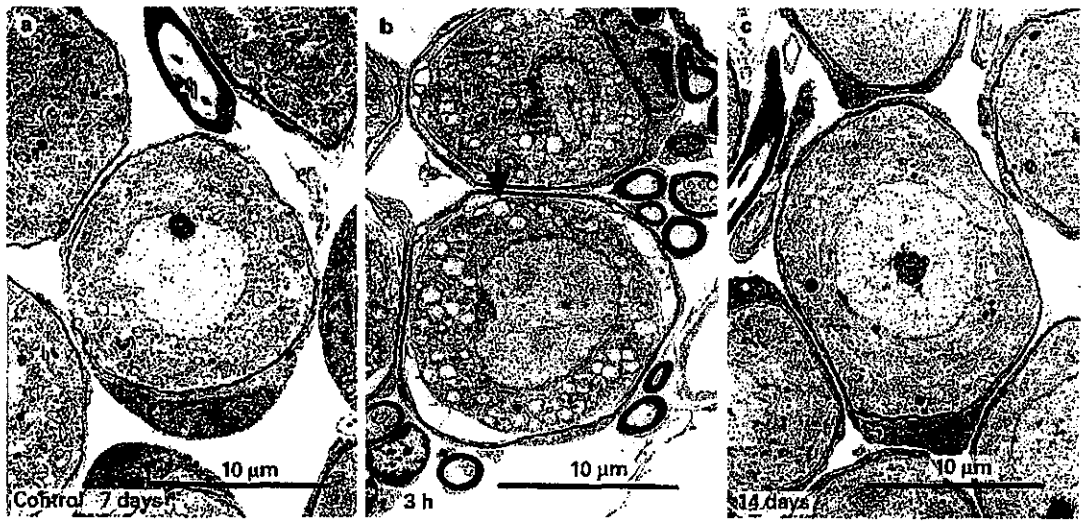

Fig. 8. Ultrastructural analysis of spiral ganglion cells after the administration of saline (**a**) or 3-NP (**b**, **c**). **a** Normal morphology in spiral ganglion cells 7 days after saline administration. **b** Mitochondrial vacuolation was prominent 3 h after 3-NP administration. **c** Mitochondria exhibited normal structures 14 days after 3-NP administration.